Multifragmentation of C_{60} by fast Li^0 atoms and Li^{1-3+} ions in electron loss and capture collisions

A. Itoh, H. Tsuchida,* T. Majima, S. Anada, A. Yogo, and N. Imanishi
Department of Nuclear Engineering, Kyoto University, Kyoto 606-8501, Japan
(Received 14 June 1999; published 8 December 1999)

Fragmentation and ionization of C_{60} are studied for electron capture and loss collisions of fast Li^{q+} ($q=0-3$) projectiles at a velocity $v=3.38$ a.u. Production cross sections are measured for all observed ions by a time-of-flight method in coincidence with outgoing projectile charge states k. Multifragmentation as well as multiple ionization are observed strongly even for the neutral projectiles. Total production cross sections, summed over all observed ions, are found to be the same order of magnitude for $q \leqslant 2$, indicating that the fragmentation is induced in close collisions, i.e., by penetration of the incident particles through the C_{60} cage. Also, it is found that the total fragmentation cross sections as a function of k show nearly the same shape as the equilibrium charge state distributions (CSD) measured for other condensed materials. This certainly implies that a memory for the initial charge state q is nearly lost while penetrating the cage, and the final CSD is approximately equilibrated.

PACS number(s): 34.70.+e, 36.40.−c

I. INTRODUCTION

In recent atomic collision researches, the free C_{60} molecule has attracted increasing attention as a promising collision partner that provides essential information about physical and chemical properties of matter lying between atoms and solids [1]. A large number of experimental studies have been made into the nature of C_{60}, used either as a projectile or a target particle, by various collision techniques including C_{60}^{r+} impact [2–7], photoabsorption [8–12], electron impact [13–18], and ion impact [19–34]. Compared to typical atomic collisions, however, interaction involving C_{60} is rather complicated because of its essential many-body property. This leads, consequently, to various many-body phenomena such as collective excitation of valence electrons observed in photoabsorption [8], or fragmentation into small-size ions C_n^+ observed in multiphoton excitation [12] and in ion-impact collisions [19–34]. In collisions with highly charged ions (HCI's) of low velocities, fragmentation is likely to be induced by Coulomb explosion of multiply ionized parent ions formed through many-electron removal by strong attractive Coulomb force from the incident HCI's [19–27]. Indeed, surprisingly high-charge states of C_{60}^{r+} ions, with r up to 60, have been observed recently by Martin *et al.* [27] in 475-keV Xe^{25+} collisions. In high-energy HCI collisions (e.g., 625-MeV Xe^{35+}) [28–30], where the electron-capture process is less important, multiply charged parent ions may be created via ionization of loosely bound valence electrons, expected in analogy to multiple ionization in typical ion-atom collisions [35]. On the other hand, it is not straightforward to understand the fragmentation phenomena observed in collisions with lowly charged medium velocity ions (e.g., He^+ and Ar^{3+} of a few hundred keV) [31–34], since neither the multiple electron transfer nor the multiple ionization are likely to occur.

It is known both experimentally and theoretically [2,4,6,7,12,36] that the fragmentation is affected significantly by the amount of internal energy of C_{60} after collisions. For instance, Campbell *et al.* [36] demonstrated that, at internal energies below about 100 eV, evaporation of neutral C_2 molecules is the dominant relaxation process of excited parent ions, and above about 220 eV the parent ions are broken into entirely small ions ($n<5$) (multifragmentation). The fragmentation by lowly charged ions mentioned above may be understood from this internal energy consideration. For low velocity collisions of 50-keV $C_{60}^{\pm}$ ions with rare atoms, where the predominant projectile energy-loss process is the elastic nuclear collisions, Lersen *et al.* calculated this energy loss using screened atomic potentials, and successfully reproduced their experimental distribution patterns of daughter ions [6]. Little is known about inelastic or electronic energy transfer between fast ions and C_{60}. The amount of such inelastic energy deposition is supposed to be different for different inelastic collisions, leading to a variety of fragmentation patterns for different collisions. It is, therefore, important to study individual collision processes separately to achieve better understanding of the fragmentation process. Walch *et al.* [19] made experiments of this kind for electron-capture processes of slow HCI's using a method of coincidence measurements between fragment ions and outgoing projectile ions. Variation of the fragmentation pattern as a function of the number of captured electrons was clearly demonstrated. Since then, similar experiments have been extensively carried out using slow [23–27] and fast HCI's [30]. Among these experiments, Martin and co-workers employed triple coincidence techniques also including the number of emitted electrons, allowing them to determine fragmentation schemes of multiply charged parent ions [24–27]. As for the high-velocity region, electron-capture and -loss processes were examined for 15.6-MeV multiply charged carbon ions [30]. In contrast, much less information is available about the C_{60} fragmentation process by lowly charged fast ions. Hence

*Present address: Department of Physics, Nara Women's University, Nara 630-8506, Japan

we have recently performed experiments for electron-capture and -loss collisions of 2-MeV lithium ions, and demonstrated dramatic changes in the fragmentation patterns for various individual charge-changing collisions [37].

In this work, we extend measurements to neutral Li^0 projectiles. This extension allows one to investigate the fragmentation process within a framework of only close collisions, because the interaction region responsible for ionization (electron loss) of a fast atom by a neutral target molecule may be practically limited to only within, e.g., the C_{60} molecular radius. The comprehensive set of cross-section data is obtained for the production of individual fragment ions and intact parent ions for almost all combinations between the incident and the outgoing charges. Using these absolute cross sections, the multifragmentation and ionization are investigated in detail for individual charge-changing collisions of direct $(q \rightarrow q)$, single-electron $(q \rightarrow q \pm 1)$, two-electron $(q \rightarrow q \pm 2)$ and three-electron $(q \rightarrow q \pm 3)$ processes. Moreover, the equilibration of charge state distributions (CSD's) is examined for outgoing particles passing through the C_{60} cage. The CSD's obtained are compared with equilibrium CSD's for different target materials of nitrogen gas [38] and thin carbon foils [39].

II. EXPERIMENT

The experiment was performed at the 1.7-MV tandem Cockcroft-Walton accelerator facility of Kyoto University. The apparatus and time-of-flight (TOF) technique are described in detail in our previous paper [37] carried out for 2-MeV $Li^{1,2,3+}$ ions, so that only a brief outline is given here. A well-collimated beam of 2-MeV Li^+ ions ($v = 3.38$ a.u.) was used as a primary beam. A small portion of the beam, neutralized via electron-capture collisions with residual gases in the beam line, was selected out of the primary beam by removing charged particles by a magnet. The neutral beam was then incident on a gas-phase C_{60} target in a crossed-beam collision chamber. Outgoing particles were charge-separated by a magnet and detected by a movable solid-state detector (SSD). A mass-to-charge analysis of fragment ions was made with a TOF spectrometer in conjunction with a two-stage multichannel plate detector (MCP). The TOF spectra were measured by the fast-multichannel scaler that is capable of counting multiple ions of different mass-to-charge ratio produced in a single collision event. A flight time of the slowest ions $C_{60}{}^+$ was about 12 μs. The base pressure was below 3×10^{-7} Torr through the whole experiment.

The C_{60} target was produced by heating 99.9% pure C_{60} powder at 500 °C in a temperature-controlled quartz oven located at the base of the collision chamber. Through a hole (2 mm in diameter) opened at the top of the oven, the C_{60} molecular beam was introduced upward into a collision region. The average target density within an observation length (4 cm) was about 5.1×10^{10} (molecules/cm^3), equivalent to 8.7×10^{-7} Torr. These calculations were made using the vapor pressure data reported by Abrefah *et al.* [40]. It is noted that the vapor pressure data scatter substantially in literatures [40–42], so that an uncertainty of the above value is supposed to be a factor of 2.

Absolute cross sections for the production of secondary ions were obtained in coincidence with outgoing projectiles of desired charge states k ranging from 0 to 3. The intensity $Y_n(qk)$ of an nth product ion in a given charge-changing collision $(q \rightarrow k)$ is written by

$$Y_n(qk) = I_0 X \sigma_n(qk) = \frac{I_{qk}(S)}{\Phi_{qk}} X \sigma_n(qk), \tag{1}$$

where I_0 is the incident beam flux, X the effective target thickness, $\sigma_n(qk)$ the production cross section, $I_{qk}(S)$ the number of outgoing particles with charge k detected by the SSD, and Φ_{qk} the outgoing charge fraction measured by moving the SSD within a whole range covering all charge states. Here the quantities $Y_n(qk)$ and X represent corrected values with respect to various factors such as the ion-collection efficiency of the TOF spectrometer, detection efficiency of the MCP, and so forth. More details of these correction factors were given in Ref. [37]. In order to increase the experimental accuracy, the total number of charged products, irrespective of coincidence or noncoincidence events, was routinely measured as a monitor of the incident beam flux I_0 which was varied appropriately for each charge-changing collision in order to minimize the SSD counting loss.

For a collision process $0 \rightarrow 0$, where no charge change takes place, the measurement was extremely difficult because nearly all of the particles detected by the SSD were those that underwent no interactions with the C_{60} target. This inhibited us from obtaining reliable cross sections with a good accuracy. However, the relevant cross sections $\sigma_n(00)$ were found, from a long-time measurement, to be smaller by more than three orders of magnitude than those for other electron-loss processes.

In the present Li^0 experiment, we also measured TOF spectra in coincidence with secondary electrons emitted simultaneously with charged products. The electrons were detected by another MCP in the opposite direction of the TOF spectrometer, and were used as the start trigger pulse; for more details the reader is directed to Ref. [18]. The TOF spectrum measured in this electron-start mode represents a total distribution including all $0 \rightarrow k$ processes, because in Li^0 collisions the secondary electrons are always emitted when the charged products are created. Absolute values of the corresponding total cross sections were, however, not measured in this work. Except for the systematic error of a factor two arising from the target desntity, overall relative experimental errors of the present cross sections are estimated to be 20–30 %.

Notations used in the following sections are summarized here. The production cross section $\sigma_n(qk)$ refers to the ''ionization cross section'' for parent ions are $C_{60}{}^{r+}$, and is rewritten by $\sigma_r(qk)$. As shown below, the TOF spectrum consists of the fragmentation part ($C_n{}^+$, $n = 1$–14) and the ionization part ($C_{(60-2m)}{}^{r+}$, $m \geq 0$, $r = 1$–4) including large daughter ions. Cross sections for these two parts are denoted $f(qk)$ and $I(qk)$, respectively, as

$$f(qk)=\sum_{n=1}^{14}\sigma_n(qk), \tag{2}$$

$$I(qk)=\sum_{r=1}^{4}(\sigma_r(qk)+\sigma_D^r(qk)), \tag{3}$$

$$T(qk)=f(qk)+I(qk) \tag{4}$$

The quantity $\sigma_D^r(qk)$ represents all observed daughter ions with charge r. The last equation is the total cross section of all observed ions. Note that the ionization cross section for $C_{60}{}^{4+}$ ions was determined by subtracting an overlapping $C_{15}{}^{+}$ peak which has always a broader peak profile than $C_{60}{}^{4+}$. The total production cross section of a given ion in a given q is obtained by summing over all values of k as

$$\sigma_i(q)=\sum_{k=0}^{3}\sigma_i(qk), \tag{5}$$

with i standing for either n or r.

III. RESULTS AND DISCUSSION

A. Spectra and cross sections

Figure 1 shows mass-to-charge distributions of fragment ions produced in electron-loss collisions of 2-MeV Li^0 atoms with the C_{60} target. The upper three figures, denoted $0\rightarrow k$ ($k=1$–3), are partial distributions corresponding to k-electron-loss collisions, and the bottom one is the total distribution obtained by the electron-start mode. By summing these partial spectra on an absolute scale, a total spectrum was constructed and was found to be almost the same as the bottom spectrum, supporting our surmise that the contribution from the direct process ($0\rightarrow 0$) is negligible in Li^0 collisions.

The most striking feature seen in Fig. 1 is that the multifragmentation and multiple ionization are both induced strongly even by the Li^0 impacts. Since the Coulomb force between two neutral particles is important only at small impact parameters, the present result certainly implies that these two processes are both induced in close collisions. Next, relative intensities between the fragmentation part ($C_n{}^{+}$, $n=1$–14) and the ionization part ($C_{(60-2m)}{}^{r+}$, $m\geqslant 0$, $r=1\sim 4$) are found to change strongly depending on the outgoing charge state k. For instance, the spectrum for $0\rightarrow 1$ is dominated by the ionization part, and that for $0\rightarrow 3$ is dominated by the fragmentation part. One can see also in the figure that the multiple ionization ($r>2$) increases with increasing k when compared the peak intensities of different r. All these experimental findings indicate that the collision becomes more violent with increasing number of electrons lost from the incident Li^0 atoms.

Cross sections $\sigma_i(0k)(i=n$ or $r)$ for the production of $C_n{}^{+}$ ($n=1$–14) and $C_{60}{}^{r+}$ ($r=1$–4) are presented in Fig. 2 as a function of n and r, respectively. Total cross sections $\sigma_i(0)$ obtained by Eq. (5) are also depicted. First to be mentioned here is that all these cross sections are significantly smaller than the geometrical C_{60} cross sections of

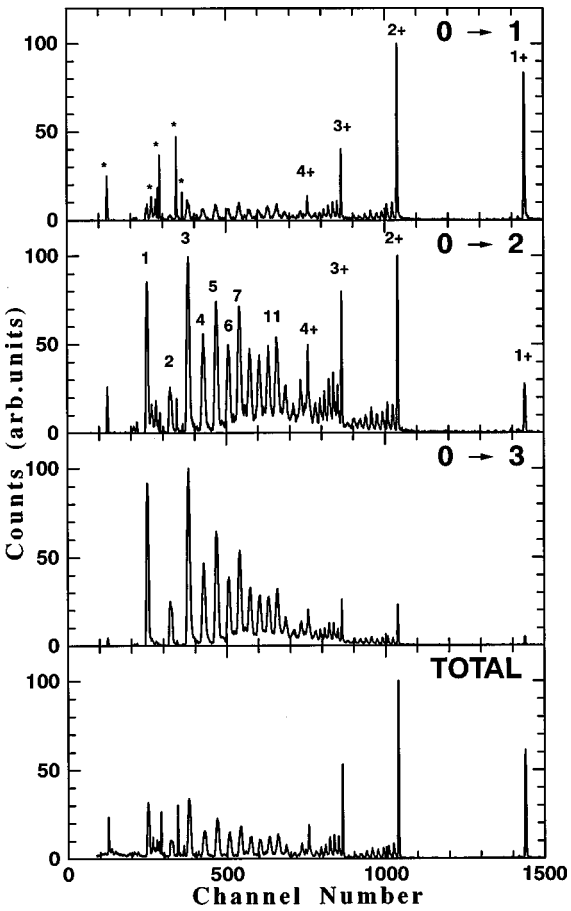

FIG. 1. Time-of-flight spectra obtained for 2-MeV Li^0 collisions with a C_{60} target. The numbers $0\rightarrow k$ represent the charge-transfer process, and the bottom spectrum denoted ''total'' is the total distribution obtained by the electron-start mode. The sharp lines (*) observed in the left part are the background peaks originating from residual gases of H_2O, N_2, and O_2.

3.8×10^{-15} cm^2 (molecular radius 6.6 a.u). This fact implies again, but quantitatively, that the fragmentation and ionization of C_{60} by Li^0 are both induced in close collisions inside the molecular cage. Total cross sections $\sigma_n(0)$ for small fragment ions are dominated by the two-loss process ($0\rightarrow 2$), accounting for about 50% of the total values. It is interesting to point out that the one-loss process gives significantly small cross sections compared to the two-loss process. On the other hand, the ionization part is completely dominated by the one-loss process, in particular for $r\leqslant 2$, and the three-loss process makes practically no contribution to the production of parent ions. It is also noted that the cross sections $\sigma_n(0k)$ in a given k, apart from well-known even-odd oscillations, do not change very much for different cluster size n. In the three-loss process, however, one can see a slight enhancement of smaller size clusters, indicating more violent collisions compared to other electron-loss processes. More detailed discussion about these experimental results is given below together with our previous cross sections for Li^{1-3+} ions.

Total production cross sections $T(qk)$ obtained by integrating all product ions in a given $q\rightarrow k$ process are shown in

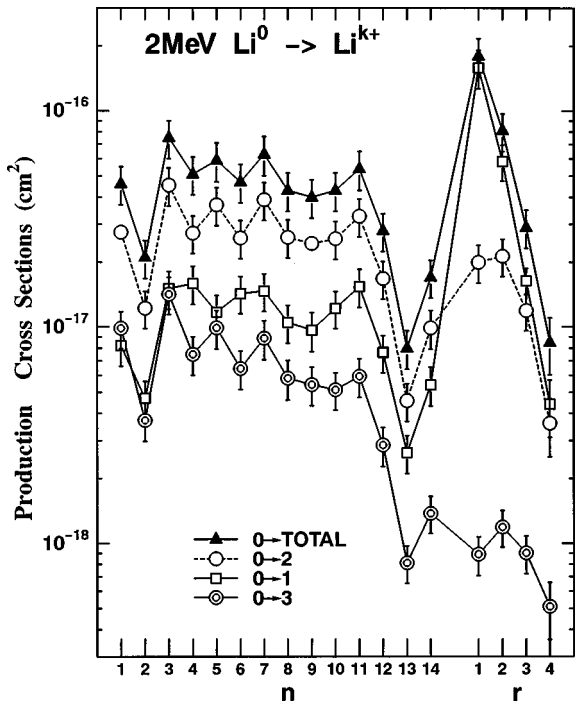

FIG. 2. Production cross sections for fragment ions C_n^+ and ionized parent ions C_{60}^{r+} measured for $0 \rightarrow k$ charge-changing collisions of Li^0. The abscissa represents the number of *n* and *r*.

Fig. 3(a) as a function of the incident charge state *q*. Fragmentation cross sections $f(qk)$ defined by Eq. (2) corresponding to the sum of small-size clusters C_n^+ $(n=1-14)$ are presented in Fig. 3(b). Here the cross sections for large daughter ions $C_{(60-2m)}^{r+}$ are included in the ionization cross sections $I(qk)$, because these ions are known to be produced predominantly via evaporation of C_2 units from parent ions [24,26,43]. Note that $T(qk) \sim f(qk)$ for three-loss $(0 \rightarrow 3)$, one-capture $(q \geq 2)$ and two-capture processes. The cross

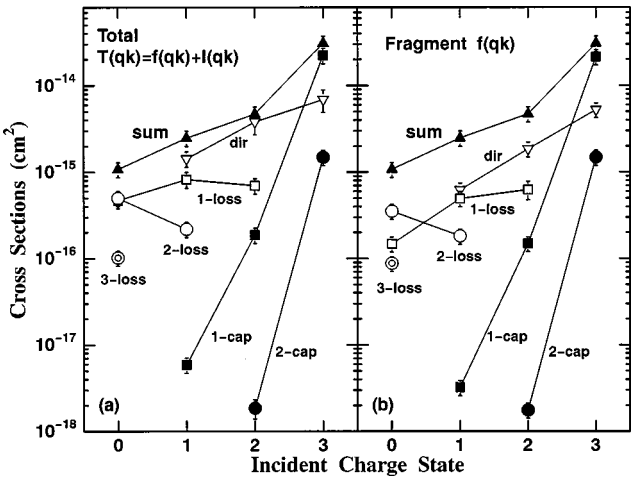

FIG. 3. Total production cross sections $T(qk)$ and fragmentation cross sections $f(qk)$ for $q \rightarrow k$ collisions as a function of the incident charge *q*. The ''sum'' cross sections (closed triangles) shown both in (a) and (b) are the sum of $T(qk)$ over the final charge state *k* in each incident charge *q*.

sections denoted ''sum'' in both figures are the sum of $T(qk)$ over *k*. One of the important experimental findings here is that the sum cross sections increase rather slowly as the incident charge increases up to $q=2$. Although our cross sections may have uncertainties of factors of about two, it is worthwhile here to note the relative values of these cross sections; they are 1, 2.3, 4.4, and 29 for $q=0-3$, respectively. Apparently, this result implies that collisions of charged projectiles with C_{60} are taking place at similar impact parameters as Li^0 collisions, resulting in equivalent influences on the target. Here the impact parameter is taken as the distance from the center of the C_{60} molecule to the incident beam.

In Fig. 3(a) one can see the number of contributions from individual charge-changing processes. In particular, the direct processes $[T(qq)]$ are found to give the largest cross sections of all collision proceses except for $q=3$, for which the one-capture process $[T(32)]$ gives the largest value. Furthermore, the ionization cross sections in direct processes, $I(qq)=T(qq)-f(qq)$, are found to be significantly large, accounting for about half the values of $T(qq)$.

For one-electron-loss processes, the total cross sections $T(qk)$ are nearly constant, while $f(qk)$ increases with increasing *q*, implying an opposite behavior of an ionization part $I(qk)$. As for the two-loss processes, all the relevant cross sections of $f(qk)$, $I(qk)$, and $T(qk)$ decrease with increasing *q*. Qualitatively, to stay within a framework of ion-atom collisions, the impact parameter (*b*) relevant to the projectile ionization (electron loss) would become smaller with increasing ionization potential of the projectile particles. Ionization potentials of Li^{q+} are 5.4, 75.6, and 122.5 eV for $q=0-2$, respectively [44]. The target ionization accompanying the projectile electron loss is accordingly expected to become smaller with decreasing *b*, resulting in smaller cross sections of $I(qk)$ at larger *q*. It is interesting to note that the cross-section ratio $T(02)/T(13)=2.3$ is in fairly god accordance with the ratio of the energy required to ionize two electrons from the projectiles; 81 eV for $0 \rightarrow 2$ and 198 eV for $1 \rightarrow 3$. On the other hand, the amount of energy deposition to the target would increase at smaller values of *b*, as found in theoretical work on atomic or diatomic molecular targets [45,46]. If we assume this argument also to be valid for the C_{60} molecule, the multifragmentation in projectile electron-loss collisions would thus increase with decreasing *b*, at which a large amount of inelastic energy may be deposited. Actually, the trend of this violent fragmentation is observed in this work, as discussed in Sec. III B.

Contrary to these direct and electron-loss processes, a dramatic *q* dependence is observed for electron-capture processes. For instance, $T(32)$ is larger than $T(10)$ by more than three orders of magnitude, and $T(31)/T(20)$ is about 800. One reason for this steep increase might be attributed to K-to-K electron transfer, where a carbon 1*s* electron is captured into a projectile 1*s* orbital. Applying the theory of this K-K transfer [47] to the present collisions system of $Li^{3+}+C$, we found that the transfer cross section reaches its maximum value ($\sim 1.5 \times 10^{-17}$ cm^2/atom) at around 2-MeV projectile energies. It is noted that this maximum value is somewhat larger than the cross sections for direct ionization

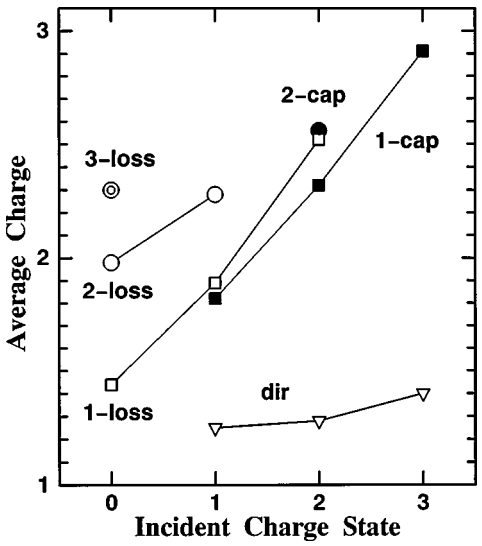

FIG. 4. Average charges of parent ions as a function of q.

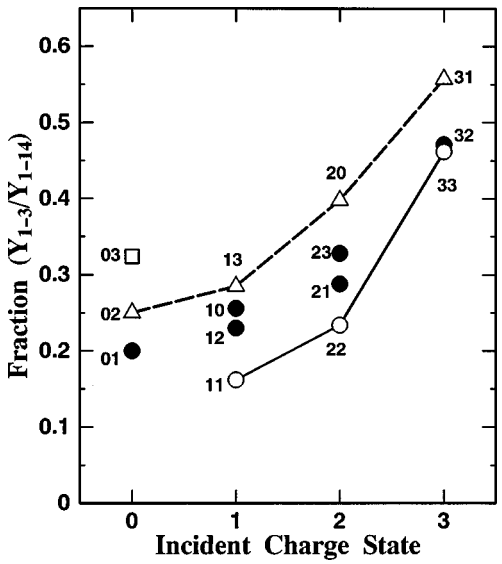

FIG. 5. Fractions of the first three (Y_{1-3}) fragment ions out of the total fragment ions (Y_{1-14}) plotted as a function of q. To guide the eye, two curves are drawn for direct processes ($q \rightarrow q$) and two electron-loss and -capture processes ($k = \pm 2$).

of carbon 1s-electron at 2 MeV [48]. Since the K-K transfer occurs predominantly at small impact parameters [47], of about target K-shell radius (0.17 a.u.), a large amount of energy deposition is expected in such collisions, resulting in further promotion of fragmentation. This close-collision effect may be the chief reason of the experimental fact of the predominant contribution of $f(qk)$ to $T(qk)$ for both one- and two-electron-capture collisions. This implies convincingly that the C_{60} molecule is preferentially disintegrated in capture collisions rather than leaving the resultant parent ion intact. This is the essentially different characteristic compared to slow HCI collisions, in which the one- or two-electron-capture process is dominated only by rather gentle distant collisions [19–27].

B. Ionization and fragmentation

As mentioned above, it is somewhat astonishing to find that C_{60} can be ionized by neutral particles. This is understandable only in close collisions where the screening of the lithium nucleus by orbital electrons becomes weak, and, consequently, it leads to the target ionization. Figure 4 shows the average charge $\bar{r}$ of parent ions, calculated by $\bar{r} = \Sigma r \sigma_r / \Sigma \sigma_r$ using ionization cross sections σ_r for C_{60}^{r+}. The values of $\bar{r}$ are found to differ significantly for different collision processes. For direct processes, $\bar{r}$ is small and nearly independent of q. This is due to the fact that, in direct processes, the predominant secondary ion is always C_{60}^{+} produced via direct ionization, and multiply charged ions decrease steeply with increasing r, as reported in our previous paper [37]. This trend is basically the same as observed in usual ion-atom collisions [35]. Hence, it is plausible to state that the direct ionization, of mostly outer-shell electrons occurs at relatively large impact parameters, resulting in large ionization cross sections as shown in Fig. 3. Contrary to these direct processes, the average charge increases from 1.4 ($0 \rightarrow 1$) to 2.5 ($2 \rightarrow 3$) for one-electron-loss processes and from 1.8 ($1 \rightarrow 0$) to 2.9 ($3 \rightarrow 2$) for one-electron-capture processes. The sharp increase in these processes implies that the multiple ionization is more preferential for larger q even in one-electron processes. In addition, the one-electron-loss processes give rise to slightly larger values of $\bar{r}$ than the corresponding one-electron-capture processes. This seems to indicate that the electron loss, or the projectile ionization by C_{60}, is the more violent collision.

Another important result is that the values of $\bar{r}$ in a given q an increase substantially with an increasing number of electrons captured by or lost from the projectiles. It is worthwhile to note that the three-loss process of Li^0 gives about $\bar{r} = 2.3$, which is equivalent to the numbers for $1 \rightarrow 3$ and $2 \rightarrow 1$ collisions. A large value of 2.9 for the $3 \rightarrow 2$ process may be understood again by the K-K transfer effect, resulting in additional electron emission following the Auger transition. Note that for the two-capture process of Li^{3+} no noticeable parent ions were produced, but only fragment ions.

As for the collision-induced C_{60}-fragmentation, the degree of fragmentation may be investigated by an analysis of the relative intensities of small fragment ions C_n^{+} in the fragmentation part. That is, the smaller ions such as $n \leqslant 3$ would be pronounced largely compared to other heavier fragments when the degree of fragmentation becomes high. This is demonstrated in Fig. 5, where the total fractions of the first three fragments (C_{1-3}^{+}) out of all fragment ions (C_{1-14}^{+}), Y_{1-3}/Y_{1-14}, are plotted as a function of q. For clarity two curves are drawn corresponding to direct ($q \rightarrow q$) and two-electron ($q \rightarrow q \pm 2$) processes, respectively. One can clearly see the following two distinctive characteristics about the C_{60} multifragmentation. First, the multifragmentation becomes significant with increasing incident charge q. The fact of nearly equivalent fractions in both one-loss and one-capture processes in a given q seems to imply that the loss and capture collisions both occur at equivalent impact parameters, resulting in a similar amount of energy deposition. This, however, does not mean equivalent fragmentation cross sec-

tions for these two processes, since the relevant probabilities may be significantly different from each other, as can be recognized from the large difference between $f(12)$ and $f(10)$ shown in Fig. 3. Second, in a given q the multifragmentation increases with an increasing number of electrons captured by or lost from the projectiles. This is the same trend as observed for multiple ionization (Fig. 4). As one interpretation of this result, we suppose that multiple-electron processes are induced preferentially by double collisions taking place at the front and back surfaces of a C_{60} molecule. Such double collisions are likely to result in smaller cross sections than those for single collisions, as shown in Fig. 3. In turn, the total amount of energy deposition would increase substantially and, consequently, more violent fragmentation may possibly be induced.

Since the energy deposition is directly related to the stopping power of the target, one can estimate the amount of energy deposition to C_{60} using usual stopping power calculations. On the basis of Bethe theory, Kaneko derived an analytical formula of stopping cross sections for fast bare, hydrogenlike, and heliumlike ions [49]. For the collision systems of 2-MeV $Li^{q+}+C$, the stopping cross sections S_e, in units of 10^{-15} eV cm^2/atom, are 31.5, 55.4, and 94.4 for $q=1$, 2, and 3, respectively. The energy deposition per C_{60} molecule may be obtained by, $E=\rho S_e$, with the surface number density, $\rho=60/\pi a^2=1.56\times10^{16}$ (atoms/cm^2), and $a=6.6$ a.u. Calculated results are 491, 864, and 1473 eV for $q=1$, 2, and 3, respectively. It should be noted that the degree of fragmentation shown in Fig. 5 has a remarkably similar trend of relative variation versus q to these calculated values. In Kaneko's paper, the charge state of the projectile ions is treated as ''frozen'' during collision and, therefore, the calculated values can be thought to correspond to direct processes ($q\rightarrow q$) in the present work. If the degree of fragmentation obtained in the present work is assumed to reflect the total amount of energy deposition, the data in Fig. 5 indicate clearly that the energy deposition in charge-changing collisions is larger than that in direct collisions. Thus this suggests that a more detailed knowledge of, for example, the impact-parameter-dependent stopping power is necessary to investigate furthermore the energy-transfer mechanism in charge-changing collisions.

C. Charge-state distribution of cage-penetrating particles

The spherical cage structure of C_{60}, consisting of 60 carbon atoms on its spherical surface of radius 6.6 a.u., readily reminds us of an intuitive picture that the molecule may act as a thin-foil target for an incoming projectile particle. Hence the charge-state distribution (CSD's) of outgoing particles appear to be important information closely related to the collision interactions involving extremely thin film targets. The thickness of a foil target is estimated from ρM_c to be 0.32 (μg/cm^2), with M_c the mass of a carbon atom. It should be noted that the C_{60} gas pressure used in our experiment is so low that almost all the outgoing projectiles pass through the target region without charge-changing collisions. It implies that the CSD, Φ_{qk} in Eq. (1), measured by the SSD is not what we are seeking. Instead, the desired quantities are the number and the charge state of particles which really penetrated the molecular cage. Such quantities may be obtained from our cross section data in the following way. First, for almost all collision processes the production cross sections of fragment ions are substantially small compared to the geometrical C_{60} cross sections. Second, various experimental findings described in the preceding sections indicate that the multifragmentation is evidently induced in close collisions within the C_{60} molecular cage. Thus the cross sections $f(qk)$ for the production of small fragment ions can reasonably be assumed to reflect the number of cage-penetrating particles of charge k. The CSD F_{qk} for these particles can then be calculated by

$$F_{qk}=\frac{f(qk)}{\sum_{k=0}^{3} f(qk)}. \tag{6}$$

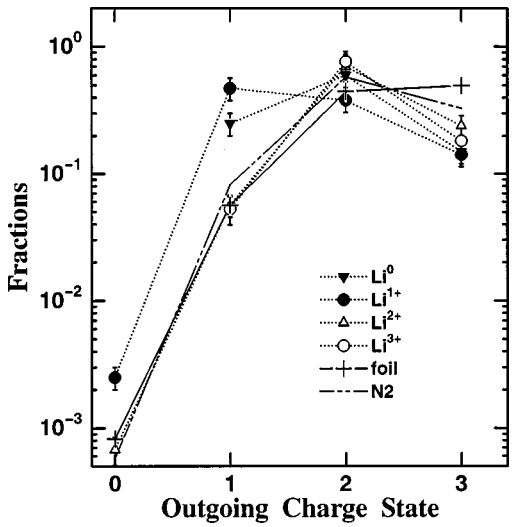

FIG. 6. Charge-state distributions in outgoing projectiles calculated from fragmentation cross sections $f(qk)$ for individual $q\rightarrow k$ processes ($k=0\sim3$). Equilibrium CSD measured for N_2 [38] and carbon foils [39] are also plotted.

The results are presented in Fig. 6 as a function of k for all $q\rightarrow k$ processes. Obviously, the overall shapes of the CSD's reveal remarkably similar distributions to each other, particularly for $q=2$ and 3. In fact, the average charge of outgoing particles, obtained by $\bar{k}=\Sigma_{k=0}^{3}kF_{qk}$, is found to differ only slightly for different incident charges; $\bar{k}$ for $q=0-3$ are 1.9, 1.7, 2.2, and 2.1, respectively, with experimental uncertainties of about 20%. This finding indicates strongly that the cage-penetrating particles can attain nearly equilibrium charge distributions. An indication of this equilibration was pointed out also by Walch *et al.* [19] in slow HCI collisions.

It is worthwhile to compare the present results with the equilibrium CSD's obtained for other target materials. The comparison is made with a nitrogen gas [38] and a carbon foil [39]. For the N_2 target the equilibrium CSD was measured in a target thickness of $(5-50)\times10^{15}$ [molecules/cm^2]. As for the carbon foil, there are no data

available in the present energy region, so that we carried out the measurements using foils of thickness 10–20 ($\mu g/cm^2$) in the projectile energy range 1–6 MeV [39]. Here we show only the results at 2 MeV. The present results for C_{60} are, in overall, in fairly good agreement with those for these targets. Average charges for the N_2 and the foil targets are 2.23 and 2.43, respectively. The former value coincides fairly well with the present values, indicating that the single C_{60} molecule seems to be almost equivalent to the thick gaseous target. On the other hand, a somewhat large value observed for the foil target is caused by a large fraction of $k=3$. It is not clear at present whether this discrepancy between C_{60} and foil targets arises from the difference of the so-called density effect [50], or is due to other reasons.

IV. CONCLUSIONS

C_{60} multifragmentation was studied experimentally for charge-changing collisions of 2-MeV Li^{0-3+} projectiles. Using neutral particles as projectiles, the fragmentation process was investigated within the framework of close collisions. To our knowledge, this is the essentially different aspect of our work compared to other experiments using highly charged slow ions, in which the distant collision likely plays the dominant role in the fragmentation processes. Production cross sections of fragment ions and intact ionized parent ions were examined as a function of the incident charge state. It was found that both multifragmentation and multiple ionization are also induced by Li^0 impacts as strong as charged projectiles. Furthermore, the total fragmentation cross section for the Li^0 beam was found to be of the same order of magnitude as those for the charged projectiles. These results evidently suggest that the fragmentation in charge-changing collisions is induced by nearly identical impact-parameter collisions. However, the details of the fragmentation are substantially different for different collision processes, indicating different amounts of inelastic energy deposition in these collisions. In particular, multifragmentation and multiple ionization are highly promoted with increasing numbers of active electrons responsible for charge-changing collisions. These multiple-electron processes are, of course, expected to accompany larger energy depositions compared to direct or one-electron capture or -loss processes.

The total amount of energy deposition was calculated using an available analytical formula for stopping cross sections [49]. Present results of the degree of fragmentation indicate that the energy deposition may be larger in charge-changing collisions in comparison with direct ($q \rightarrow q$) collisions.

The various experimental findings convincingly illustrate the following conclusion. In collisions with fast and low-charge ($q \leqslant 3$) projectiles, C_{60} multifragmentation is induced predominantly by the cage-penetrating particles. Assuming the number of such particles to be proportional to the fragmentation cross sections, the charge-state distribution in the outgoing beams was examined. The obtained distributions were found to have profiles similar to each other among different incident charge states and also to equilibrium CSD's in N_2 and carbon foil targets. We conclude, therefore, that a single C_{60} molecule is nearly identical to a dense material in which the equilibration of the CSD's is attained. In order to examine this property more precisely, however, it is necessary to carry out systematic experiments using various projectile ions with different velocities and charge states.

ACKNOWLEDGMENTS

We gratefully acknowledge Dr. Y. Nakai at RIKEN. We also thank M. Imai, K. Yoshida, and K. Norizawa for their valuable suggestions and technical support during this experiment.

[1] H. Haberland, in *Clusters of Atoms and Molecules*, edited by J. Peter Toennies, Chemical Physics Vol. 52 (Springer, Berlin, 1994).
[2] P. Hvelplund, L.H. Andersen, H.K. Haugen, J. Lindhard, D.C. Lorents, R. Malhotra, and R. Ruoff, Phys. Rev. Lett. **69**, 1915 (1992).
[3] C. Brink, L.H. Andersen, P. Hvelplund, and D.H. Yu, Z. Phys. D: At., Mol. Clusters **29**, 45 (1994).
[4] H. Shen, P. Hvelplund, D. Mathur, A. Bárány, H. Cederquist, N. Selberg, and D.C. Lorents, Phys. Rev. A **52**, 3847 (1995).
[5] N. Selberg, A. Bárány, C. Biedermann, C.J. Setterlind, H. Cederquist, A. Langereis, M.O. Larsson, A. Wännström, and P. Hvelplund, Phys. Rev. A **53**, 874 (1996).
[6] M.C. Lersen, P. Hvelplund, M.O. Larsson, and H. Shen, Eur. Phys. J. D **5**, 283 (1999).
[7] R. Ehlich, M. Westerburf, and E.E.B. Campbell, J. Chem. Phys. **104**, 1900 (1996).
[8] I.V. Hertel, H. Steger, J. de Vries, B. Weisser, C. Menzel, B. Kamke, and W. Kamke, Phys. Rev. Lett. **68**, 784 (1992).
[9] T. Drewello, W. Krätschmer, M. Fieber-Erdmann, and A. Ding, Int. J. Mass Spectrom. Ion Processes **124**, R1 (1993).
[10] H. Hohmann, C. Callegari, S. Furrer, D. Grosenick, E.E.B. Campbell, and I.V. Hertel, Phys. Rev. Lett. **73**, 1919 (1994).
[11] S. Aksela, E. Nõmmiste, J. Jauhiainen, E. Kukk, J. Karvonen, H.G. Berry, S.L. Sorensen, and H. Aksela, Phys. Rev. Lett. **75**, 2112 (1995).
[12] S. Hunshe, T. Starczewski, A. I'Huillier, A. Persson, C.-G. Wahlstöm, B. Van Linden van den Heuvell, and S. Svanberg, Phys. Rev. Lett. **77**, 1966 (1996).
[13] R. Völpel, G. Hofmann, M. Steidl, M. Stenke, M. Schlapp, R. Trassl, and E. Salzborn, Phys. Rev. Lett. **71**, 3439 (1993).
[14] P. Scheier and T.D. Märk, Phys. Rev. Lett. **73**, 54 (1994).
[15] T.D. Märk and P. Scheier, Nucl. Instrum. Methods Phys. Res. B **98**, 469 (1995).
[16] B. Dünser, M. Lezius, P. Scheier, H. Deutsch, and T.D. Märk, Phys. Rev. Lett. **74**, 3364 (1995).
[17] S. Matt, B. Dünser, M. Lezius, H. Deutsch, K. Becker, A. Stamatovic, P. Scheier, and T.D. Märk, J. Chem. Phys. **105**, 1880 (1996).

[18] A. Itoh, H. Tshuchida, K. Miyabe, T. Majima, and N. Imanishi, J. Phys. B **32**, 277 (1999).
[19] B. Walch, C.L. Cocke, R. Voelpel, and E. Salzborn, Phys. Rev. Lett. **72**, 1439 (1994).
[20] J. Jin, H. Khemliche, H. Prior, and Z. Xie, Phys. Rev. A **53**, 615 (1996).
[21] J.-P. Briand, L. de Billy, J. Jin, H. Khemliche, M.H. Prior, Z. Xie, M. Nectoux, and D.H. Schneider, Phys. Rev. A **53**, R2925 (1996).
[22] T. Bergen, X. Biquard, A. Breac, F. Chandezon, C. Guet, and B.A. Huber, in *Photonic, Electronic and Atomic Collisions*, edited by F. Aumayr and H. Winter (World Scientific, Singapore, 1998), p. 657.
[23] T. Schlathölter, R. Hoekstra, and R. Morgenstern, J. Phys. B **31**, 1321 (1998).
[24] S. Martin, L. Chen, A. Denis, and J. Désesquelles, Phys. Rev. A **57**, 4518 (1998).
[25] S. Martin, J. Bernard, L. Chen, A. Denis, and J. Désesquelles, Eur. Phys. J. D **4**, 1 (1998).
[26] L. Chen, J. Bernard, A. Denis, S. Martin, and J. Désesquelles, Phys. Rev. A **59**, 2827 (1999).
[27] S. Martin, Li Chen, A. Denis, and J. Désesquelles, Phys. Rev. A **59**, R1734 (1999).
[28] T. LeBrun, H.G. Berry, S. Cheng, R.W. Dunford, H.H. Esbensen, D.S. Gemmell, E.P. Kanter, and W. Bauer, Phys. Rev. A **72**, 3965 (1994).
[29] S. Cheng, H.G. Berry, R.W. Dunford, H. Esbensen, D.S. Gemmell, E.P. Kanter, T. LeBrun, and W. Bauer, Phys. Rev. A **54**, 3182 (1996).
[30] Y. Nakai, A. Itoh, T. Kambara, Y. Bitoh, and Y. Awaya, J. Phys. B **30**, 3049 (1997).
[31] A. Itoh, H. Tsuchida, K. Miyabe, M. Imai, and N. Imanishi, Nucl. Instrum. Methods Phys. Res. B **129**, 363 (1997).
[32] A. Reinköster, U. Werner, and H.O. Lutz, Europhys. Lett. **43**, 653 (1998).
[33] H. Tshuchida, A. Itoh, Y. Nakai, K. Miyabe, and N. Imanishi, J. Phys. B **31**, 5383 (1998).
[34] T. Schlathölter, O. Hadjar, R. Hoekstra, and R. Morgenstern, Phys. Rev. Lett. **82**, 73 (1999).
[35] See, for instance, C.L. Cocke and R.E. Olson, Phys. Rep. **205**, 153 (1994).
[36] E.E.B. Campbell, T. Raz, and R.D. Levine, Chem. Phys. Lett. **253**, 261 (1996).
[37] A. Itoh, H. Tsuchida, T. Majima, and N. Imanishi, Phys. Rev. A **59**, 4428 (1999).
[38] V.S. Nikolaev, I.S. Dmitriev, L.N. Fateeva, and Ya.A. Teplova, Sov. Phys. JETP **12**, 627 (1961).
[39] A. Itoh, H. Tsuchida, T. Majima, A. Yogo and H. Ogawa, Nucl. Instrum. Methods Phys. Res. B **159**, 22 (1999).
[40] J. Abrefah, D.R. Olander, M. Balooch, and W.J. Siekhaus, Appl. Phys. Lett. **60**, 1313 (1992).
[41] C.K. Mathews, M. Sai Baba, T.S. Lakshmi Narasimhan, R. Balasubramanian, N. Sivaraman, T.G. Srinivasan, and P. Vasudeva Rao, J. Phys. Chem. **96**, 3566 (1992).
[42] V. Piacente, G. Gigli, P. Scardala, A. Giustini, and D. Ferro, J. Chem. Phys. **99**, 14 052 (1995).
[43] M. Foltin, O. Echt, P. Scheier, B. Dünser, R. Wörgötter, D. Muigg, S. Matt, and T.D. Märk, J. Chem. Phys. **107**, 6246 (1997).
[44] *CRC Handbook of Chemistry and Physics*, 67th ed. (CRC, Boca Raton, FL, 1987)
[45] C.L. Cocke, Phys. Rev. A **20**, 749 (1979).
[46] N.M. Kabachnik, V.N. Kondratyev, Z. Roller, and H.O. Lutz, Phys. Rev. A **56**, 2848 (1997); **57**, 990 (1998).
[47] G. Lapicki and F.D. McDaniel, Phys. Rev. A **22**, 1896 (1980).
[48] G. Basbas, W. Brandt, and R. Laubert, Phys. Rev. A **17**, 1655 (1978).
[49] T. Kaneko, Phys. Rev. A **43**, 4780 (1991).
[50] H.D. Betz, Rev. Mod. Phys. **44**, 465 (1973).